Mechanism for linear and nonlinear optical effects in β-BaB_2O_4 crystals

Jiao Lin*
Fujian Institute of Research on the Structure of Matter, Academia Sinica, P.O. Box 143, Fuzhou, Fujian 350002, China

Ming-Hsien Lee
Department of Physics, Tamkang University, Tamsui, Taipei 251, Taiwan

Zhi-Ping Liu and Chuangtian Chen
Fujian Institute of Research on the Structure of Matter, Academia Sinica, P.O. Box 143, Fuzhou, Fujian 350002, China

Chris J. Pickard†
National Center for High Performance Computing, P.O. Box 19-136, HsinChu, Taiwan
(Received 18 November 1998; revised manuscript received 11 June 1999)

Electronic structure calculations of β-BaB_2O_4 from first principles are performed based on a plane-wave pseudopotential method, and the linear optical properties are then obtained. The static second-harmonic generation (SHG) coefficients are calculated at the independent-particle level with a formalism originally given by Aversa and Sipe [Phys. Rev. B **52**, 14 636 (1995)] and later rearranged by Rashkeev *et al.* [Phys. Rev. B **57**, 3905 (1998)] to explicitly show Kleinman's symmetry. The formalism is improved to be more efficient in reducing the k points necessary for convergence. A real-space atom-cutting method is suggested to analyze the respective contributions of various transitions among ions and ion groups to optical response. The contribution of the cation Ba to SHG effects is found to be not important but non-negligible, while its contribution to birefringence is negligible. [S0163-1829(99)13839-6]

I. INTRODUCTION

The development of highly efficient nonlinear optical (NLO) crystals is of great importance to extend the frequency range provided by normal laser sources into the ultraviolet (UV) and infrared (IR) regions. Therefore, the search for new NLO crystals is still very active, even though intensive efforts in this field have been in progress for more than 30 years. Obviously, a full understanding of the mechanism of NLO effects in crystals is helpful to search and design new NLO crystals more efficiently. A model known as the ''anionic group theory''[1] was proposed by Chen's group to study the optical properties of NLO crystals and has proven to be highly successful in searching for and designing NLO crystals.[2] In addition to the discovery of the widely used β-BaB_2O_4 (BBO) (Ref. 3) and LiB_3O_5 (LBO) (Ref. 4), Chen's group is now developing another series of borate crystals, the SBBO family,[5] aiming for the vacuum ultraviolet (vuv) application with the assisstance of this model. Understanding the applicability of this approximation model may give a deeper insight into the mechanism of NLO effects and materials engineering. To this end (i) an *ab initio* electronic/band structure calculation is crucial to describe the extended solid, although anionic group calculations achieve preliminary success; (ii) theoretical calculations of SHG coefficients based on such band structures are required to directly determine the NLO properties of crystals, so that the various factors that may affect such quantities can be analyzed later on; and (iii) a method that can separate the respective contribution of each local subsystem of the electronic structure is needed for a comprehensive understanding of the mechanism of both linear and nonlinear optical responses.

β-barium borate (BBO), the first borate series crystal widely used in second-harmonic generation (SHG), plays a very important role in the understanding of the NLO effects because of its high performance with regard to optical properties, such as large SHG coefficients, a wide transparent and phase matchable region, good optical quality, and a high damage threshold. However, there are still controversies about the origin of its large SHG coefficient; i.e., which plays the more important role in second-harmonic generation, the Ba^{2+} cation or the $(B_3O_6)^{3-}$ anionic group?

As early as in 1976, Chen suggested[6] an anionic group model to explain the relationship between the microscopic structure of a nonlinear optical crystal and its macroscopic nonlinear optical effects, before BBO was discovered.[3] Applying such a theory to BBO with the complete neglect of differential overlap (CNDO/S) approximation, they obtained SHG coefficients that agree well with experimental values,[7] and indicated that d_{22}, the largest SHG coefficient of BBO, is mostly determined by the contribution of the $(B_3O_6)^{3-}$ anionic group, whereas the other two small coefficients, d_{33} and d_{31}, are mostly determined by the Ba^{2+} cations. Wu and Chen[9] used the discrete variational $X\alpha$ (DV-$X\alpha$) method[8] to calculate the linear optical response based on the anionic group theory, and found that although the Ba^{2+} cation contributes to both n_o and n_e of BBO, it has little influence on the birefringence $\Delta n = |n_o - n_e|$. This calculation suggests that the anionic groups are responsible for the dominant contribution to birefringence in BBO. However, the calculations mentioned above are based on localized molecular-orbital methods and have resulted in much discussion.

In 1990, French, Ling, Ohuohi, and Chen used the DV-$X\alpha$ method to explain the opto-electronic spectrum of BBO and indicated that the valence band (VB) of BBO is mainly determined by the localized orbital of the $(B_3O_6)^{3-}$ group.[10] Hsu and Kasowski first calculated the electronic-energy band structures of BBO from first principles using the *ab initio* pseudofunction method.[11] From the partial density of states (PDOS) analysis they related the band gap to the transition from the orbital of the $(B_3O_6)^{3-}$ anionic group to that of the Ba^{2+} cation, so they questioned the validity of the anionic group model. Xu *et al.* reported the electronic structure and linear optical property calculations of BBO using the first-principles orthogonalized linear combination of atomic orbitals (OLCAO) method.[12] They suggested that the anisotropies in the layered $(B_3O_6)^{3-}$ structure are the origin of the large nonlinear optical coefficient. Cheng *et al.*[13] used the CNDO/S-CI (complete neglect of differential overlap with spectral parameter suitable for the planar molecular geometry and configuration interaction) method to calculate the $Ba_3(B_3O_6)_2$ group and supposed that the charge transfer from anion O^{2-} to cation Ba^{2+} dominated the origin of its SHG coefficient. Li, Duan, and co-workers were the first to apply energy band theory to systematically study the optical properties of some NLO crystals, including BBO.[14,15] They used the linearized augmented plane-wave (LAPW) method to calculate the band structure of BBO and the PDOS for valence bands (VB's) and conduction bands (CB's) of BBO.[14] Their analysis indicated that the VB's of BBO are mainly composed of the atomic orbital of the $(B_3O_6)^{3-}$ group, while the bottom of the CB is mostly due to the Ba^{2+} orbital, especially the 6*s* orbital. Based on the band structures calculated, the linear[14] and nonlinear[15] optical properties were obtained. By comparing the calculated linear optical absorption spectra of BBO, LiB_3O_5, and $C_5B_3O_5$,[14] and by the spectral and spatial decomposition of the SHG coefficients,[15] they supposed that, although heavy cations dominate the bottom of the CB, their influence on optical response is less than that of the B-O anionic groups. However, their deduction has the following deficiencies. (i) Concerning the linear optical response, they presented their conclusion to be only one possible explanation of the difference between the absorption spectra of BBO and that of LBO or CBO. (ii) Concerning the NLO response, the methodology they adopted does not show Kleinman symmetry in the static limit; and in the SHG calculations three energy states must be considered, but they only decomposed one of them.

Consequently, although these endeavors help us in our understanding of the origin of the optical properties of BBO, we believe that a more direct picture of its optical response, both linear and nonlinear, may be given with the combination of the three essential elements proposed in the beginning of this section. In addition to overcoming the difficulty of the *ab initio* electronic structure calculation of BBO, which has a very large unit cell ($a=b=c=8.38$ Å), and the complexity of calculation for the second-order nonlinear optical response based on electronic structure calculation, we present a way to clarify the vagueness in how to extract the contribution of each individual atom or cluster from the total response.

In this paper, we carry out the calculations of refractive indexes, birefringence, and SHG coefficients of BBO based on *ab initio* pseudopotential electronic structure calculation, because this information is essential to the design of a useful SHG crystal. A real-space atom-cutting scheme is invented to analyze quantitatively the respective contributions of the cation and anionic group to various optical properties. One can then clearly find out the role the cation and the anionic group play in the optical response.

The methodology for electronic structure calculation, evaluation of optical properties, and the real-space cutting are presented and tested in Sec. II. In Sec. III, there is an extended discussion and analysis of the mechanism of the optical response of BBO.

II. METHODS AND COMPUTATIONAL DETAILS

A. Electronic structures and linear optical properties

CASTEP,[16,17] a plane-wave pseudopotential total energy package, is used for solving the electronic and band structures as well as linear optical properties of BBO with the local-density approximation (LDA) (Ref. 18) based on density-functional theory (DFT).[19] Within such a framework, the preconditioned conjugate gradient (CG) band-by-band method[17] used in CASTEP ensures a robust and efficient search of the energy minimum of the electronic structure ground state. The optimized pseudopotential[20–22] in the Kleinman-Bylander[23] form of Ba, B, and O allows us to use a small plane-wave basis set without compromising the accuracy required by our current study. Furthermore, the 5*s*,5*p* together with the 6*s* electrons of Ba are treated as valence electrons in the peusodopotential to ensure that Ba is described accurately enough without applying a nonlinear core correction,[24] as will be seen in Sec. III. These shallow core states of Ba lie in the range of valence bands dominated by the B_3O_6 group. Treating them explicitly guarantees the proper representation of the interaction that may occur between the anionic group and the cation. The efficiency of the pseudopotential optimization scheme here allows us to use such a Ba^{10+} ionic pseudopotential at a cutoff energy of less than 500 eV. The rather soft and optimized O pseudopotential that has been tested in various systems[25] enables us to use a kinetic-energy cutoff of 500 eV, which is used throughout the calculations. Its reliability will be further demonstrated in Sec. III by the results of the linear optical properties calculation. The primitive unit cell of BBO ($a=b=c=8.38$ Å, $\alpha=\beta=\gamma=96.7$) containing 42 atoms is adopted in the calculation. The electronic structure calculation of BBO is performed on the Γ point. After the ground-state charge-density calculation converges, a finer *k* points sampling titled by denser *k*-point sets[17] that reduced to six *k* points in the irreducible Brillouin zone (IBZ) with 240 extra empty bands is used for the band wave-function calculation. Such a choice of *k* sampling and the number of empty bands is based on routine calculations where satisfying convergence is always achieved. The Read and Needs[26] correction is implemented to ensure accurate optical matrix elements calculations for our nonlocal pseudopotential based method.

It is well known that the band gap calculated by the LDA is in general smaller than the experimental data. This error is due to the discontinuity of exchange-correlation energy. Therefore, a scissors operator[27,28] is usually introduced to shift all the conduction bands in order to agree with the measured value of the band gap. Assuming that the $\mathbf{r}_{mn}$ matrix

elements are unchanged, the momentum matrix elements should be renormalized regarding the change of the Hamiltonian in a way given by[29]

$$\mathbf{p}_{nm} \rightarrow \mathbf{p}_{nm} \frac{\omega_{nm} + \Delta/\hbar(\delta_{nc} - \delta_{mc})}{\omega_{nm}}, \tag{1}$$

where the subscript c in the Kroneckers represents conduction band, and the $(\delta_{nc} - \delta_{mc})$ factor restricts the correction to pairs of bands only involving one valence and one conduction-band state.

When calculating the linear optical properties, the imaginary part of the dielectric function is given by

$$\mathrm{Im}[\epsilon_{ij}(\omega)] = \frac{e^2}{\pi m^2 \hbar} \sum_{mn} \int d\mathbf{k} \frac{f_{nm} p^i_{nm} p^j_{mn}}{\omega^2_{nm}} \delta(\omega_{nm} - \omega), \tag{2}$$

where $f_{nm} = f_n - f_m$, and f_n, f_m are Fermi factors. The real part of the dielectric function is obtained by the Kramers-Kronig transform.

B. SHG coefficients

Early in 1963, Butcher and McLean[30] presented the formalism to calculate SHG coefficients based on band structure. However, due to the difficulty in dealing with the explicit divergence in the static limit of their formula, the calculation was not practical, until recently when some groups[31–39] greatly improved the evaluation methods. After Aspnes[31] gave a formalism free of divergence in cubic crystals, Ghahramani, Moss, and Sipe[32] took another important step to present a general approach to avoid the divergence by a new sum rule. Afterwards, Sipe and Ghahramani[33] improved the methodology by systematic separation of interband and intraband motion. Aversa and Sipe[34] used the length-gauge instead of velocity gauge in their formulation to give expressions lacking the unphysical divergence. Rashkeev *et al.*[39] rearranged the formalism given by Aversa to make the symmetries of $\chi^{(2)}$ more apparent. Very recently, Duan *et al.*[15] presented an evaluation technique to reduce the number of k points needed for convergence for the formula given by Ghahramani *et al.*[32]

On the other hand, in their calculations of the static $\chi^{(2)}$, Levine and Allan developed a method that includes self-consistently the local-field effects.[35–37] However, their final formulation is quite complex and therefore not easily related to the underlying electronic states. Dal Corso, Mauri, and Rubio[38] gave an alternate formalism based on the time-dependent density functional theory, avoiding the problems with the definition of the position operator for a periodic system by going to a Wannier function representation, which succeeded for some cubic semiconductors.

It is well known that when the energy of the incident photon is far less than the energy gap, the dispersion of SHG coefficients is very small. Thus only the static limit of SHG coefficients need be calculated. Furthermore, the local-field effects are found to be generally only of the order of 10% for conventional semiconductors in the static limit,[36] so we need not take them into account. We choose the formula given by Rashkeev *et al.*[39] since it is easier to relate the calculated results to the contribution of various states. Another important advantage of this formula is that it shows Kleinman symmetry automatically in the static limit. However, compared with the formula adopted by Duan *et al.*,[15] it also has a disadvantage for it needs many more k points to achieve convergence in calculating the SHG coefficients. For example, in the case of zinc-blende GaAs, 300–500 k points in IBZ[39] are needed to obtain convergence within 5%, while Duan[15] has improved the formula in Ref. 32 to be able to reach convergence within 2% by 28 k points in IBZ. He found[15] that the sum of two diverging terms in Eqs. (2.10) and (2.11) of Ref. 32 will reach a nondiverging limit, and he then replaces the summation with this limitation when $E_{ji} - 2E_{li}$ or $E_{ji} - 2E_{jl}$ is very small. Therefore, the formula given by Rashkeev must be improved to be more efficient to make possible the calculation of the SHG coefficients of BBO.

Different from the formula in Ref. 32, the formula of $\chi^{(2)}$ in the static limit derived by Rashkeev *et al.*[39] diverges when the bands are nearly degenerate. Although, when this happens one could always choose the wave function ψ_n and ψ_m in such a way that $\mathbf{r_{nm}}$ or $\mathbf{p_{nm}}$ vanishes,[34] the error in the energy level and momentum matrix elements may be aggravated when E_m and E_n are close but not equal. We solve this problem by slightly rearranging the terms to eliminate those denominators that may cause divergence, so that we obtain

$$\chi^{\alpha\beta\gamma} = \chi^{\alpha\beta\gamma}(\mathrm{VE}) + \chi^{\alpha\beta\gamma}(\mathrm{VH}) + \chi^{\alpha\beta\gamma}(\text{two bands}), \tag{3a}$$

where

$$\chi^{\alpha\beta\gamma}(\mathrm{VH}) = \frac{e^3}{2\hbar^2 m^3} \sum_{vv'c} \int \frac{d^3k}{4\pi^3} P(\alpha\beta\gamma) \mathrm{Im}[p^\alpha_{vv'} p^\beta_{v'c} p^\gamma_{cv}] \left(\frac{1}{\omega^3_{cv} \omega^2_{v'c}} + \frac{2}{\omega^4_{vc} \omega_{cv'}} \right), \tag{3b}$$

$$\chi^{\alpha\beta\gamma}(\mathrm{VE}) = \frac{e^3}{2\hbar^2 m^3} \sum_{vcc'} \int \frac{d^3k}{4\pi^3} P(\alpha\beta\gamma) \mathrm{Im}[p^\alpha_{vc} p^\beta_{cc'} p^\gamma_{c'v}] \left(\frac{1}{\omega^3_{cv} \omega^2_{vc'}} + \frac{2}{\omega^4_{vc} \omega_{c'v}} \right), \tag{3c}$$

and

$$\chi^{\alpha\beta\gamma}(\text{two bands}) = \frac{e^3}{\hbar^2 m^3} \sum_{vc} \int \frac{d^3k}{4\pi^3} P(\alpha\beta\gamma) \frac{\mathrm{Im}[p^\alpha_{vc} p^\beta_{cv} (p^\gamma_{vv} - p^\gamma_{cc})]}{\omega^5_{vc}}. \tag{3d}$$

TABLE I. Calculated values of the static $\chi^{(2)}$ for the zine-blende semiconductor GaAs (in pm/V) for different cutoff energies of the conduction bands. All results are obtained using 10 k points in IBZ.

Cutoff energy for conduction bands (eV)	6.00	7.00	8.00	9.00	10.00	11.00	12.00	13.00	14.00
$\chi^{(2)}$	118.5	132.6	137.2	144.1	154.3	160.5	162.5	162.9	164.1

Here, α, β, and γ are Cartesian components, v and v' denote valence bands, and c and c' denote conduction bands. $P(\alpha\beta\gamma)$ denotes full permutation and explicitly shows the Kleinman symmetry of the SHG coefficients. The band energy difference and momentum matrix elements are denoted as $\hbar\omega_{ij}$ and p_{ij}^{α}, respectively, and they are all implicitly **k** dependent. In the same manner, we find that the frequency-dependent formalism derived from the length gauge approach[34] can be reduced to the formalism derived from the momentum gauge approach.[32] This equivalence has been pointed out by Sipe and Ghahramani.[33]

C. Real-space atom-cutting methodology

In order to analyze the contribution of the electronic subsystem, we present here an approach that is different from that of Duan *et al.*,[15] to show the contributions of cations and anionic groups more directly. We divide the real space into individual zones, each of which contains an ion. When we set the band wave function to zero in the zones that belong to a specific ion or a cluster (which we refer to as ''cutting''), the contribution of the ion or cluster is believed to be cut away. Therefore, the contribution of an ion or an ion group is extracted when we cut other ions from the total wave functions. For example, if the contribution of ion A to the nth-order polarizabilities is denoted as $\chi^{(n)}(A)$, we can obtain it by cutting all ions except A from the original wave functions, i.e., $\chi^{(n)}(A)=\chi^{(n)}$ (all ions except A are cut). Furthermore, various manners of cutting can result in contributions of various transitions; e.g., we can find the contribution of transitions from a Ga atomic orbital in the valence bands to the As atomic orbital in conduction bands to the optical properties of GaAs by cutting As wave functions from valence bands and cutting Ga wave functions from the conduction bands.

For simplicity, we define the zones to be spheres centered on the specific ion. A natural way to define the boundary of two nearest ions is to search the points at which the charge density in the real space reaches a local minimum. According to this strategy, the cutting radius of two nearest ions can be determined. We will realize our strategy to find the cutting radius of Ba, B, and O in Sec. III.

D. Test of our evaluation methods

Although BBO is our main objective, we test our methodology by applying it to the well-studied zinc-blende semiconductor GaAs. The calculated SHG coefficient χ_{123} of GaAs is 164.7 pm/V, which agrees well with the experimental value 162 pm/V.

TABLE II. Calculated values of the static $\chi^{(2)}$ for the zinc-blende semiconductor GaAs (in pm/V) with different k points sampling. All results are obtained using 15 eV as the cutoff energy for the conduction bands.

k points in IBZ	10	20
$\chi^{(2)}$	165.8	164.7

The factors that may influence the results for SHG coefficients include the number (or maximum energy) of empty bands and the number of k points used in calculation. The tests are presented in Tables I and II. From Table I we find that for GaAs the difference for SHG coefficients between $E_{cutoff}(\mathrm{CB})=10$ eV and $E_{cutoff}(\mathrm{CB})=14$ eV is only 7%. It can be concluded that the energy states in low conduction bands are much more important for SHG effects than those in higher bands. Table II shows the convergence test for k points in IBZ. One can find that the number of k points required for convergence in our calculations is less than that of Duan.[16] In our opinion, the reason is that in his calculation of full-frequency-dependent SHG coefficients, extra errors may result from the replacement of the sum of two diverging quantities by an unchanged value.

In order to investigate the error induced by the cut edge in our real-space atom-cutting wave-function method, we perform a test by cutting a thin shell from the total wave functions of GaAs. If the surface effect is prominent in the contribution of the shell to the total response, it will become more and more dominant when the thickness of the shell becomes smaller and smaller. However, in Table III, we find that when we decrease the thickness of the shell cut, the linear and nonlinear optical quantities extrapolate to a change of no more than 5%, which will not in any way affect scientific conclusions in our studies.

To further demonstrate the validity of our cutting strategy, we cut the wave functions and calculate the corresponding linear optical properties under various cutting manners. The results are presented in Table IV. For example, the contribution of transitions from the Ga atomic orbital in the VB to the Ga atomic orbital in the CB is achieved by cutting As from all wave functions. We find that the contribution of the interatomic transition is far smaller than the intratomic transition. This result is consistent with our belief that the mo-

TABLE III. The surface effect in the real-space atom-cutting method shown by cutting shells centered at As ions in the zinc-blende semiconductor GaAs. The optical properties are calculated in different cut shell thicknesses. The distance from the center of the shell to the center of the ion is randomly set to be 1.2 Å.

Shell thickness (Å)	$\epsilon(0)$	$\chi^{(2)}_{123}$ (pm/V)
0.2	7.2758	98.3
0.15	8.0632	110.1
0.1	9.0792	125.1
0.05	10.0367	140.9
0.02	11.2663	159.5
0.002	11.2663	159.5
No cut	11.6305	165.8

TABLE IV. Test of real-space atom-cutting methodology by applying it to GaAs to calculate the static dielectric constant calculated cut wave functions. The cutting radii for Ga and As are 1.1 Å and 1.4 Å, respectively.

Manners of cutting	$\epsilon(0)$
Ga cut from all bands	7.6782
As cut from all bands	3.1310
Ga cut from VB and As cut from CB	1.2061
As cut from VB and Ga cut from CB	1.4895
Original	11.5181

mentum matrix elements of on-site transitions are much larger than that of off-site transitions. It also testifies that the optical properties can be divided into the contributions of the individual subsystems.

III. RESULTS AND DISCUSSIONS

A. The band gap of BBO

The calculated band structure of BBO in the primitive unit cell is plotted along symmetry lines in Fig. 1. We also carry out a band-structure calculation by replacing optimized pseudopotentials with ultrasoft pseudopotentials (see Fig. 2). One can find that the two band structures are similar. In both band structures, BBO is an indirect gap crystal and the direct gap at Γ is 0.08 eV larger than the indirect band gap. The similarity is not surprising; in the DFT scheme, although the calculated band gap does not correspond to the band gap in quasiparticle picture, the energy band profiles are correct,

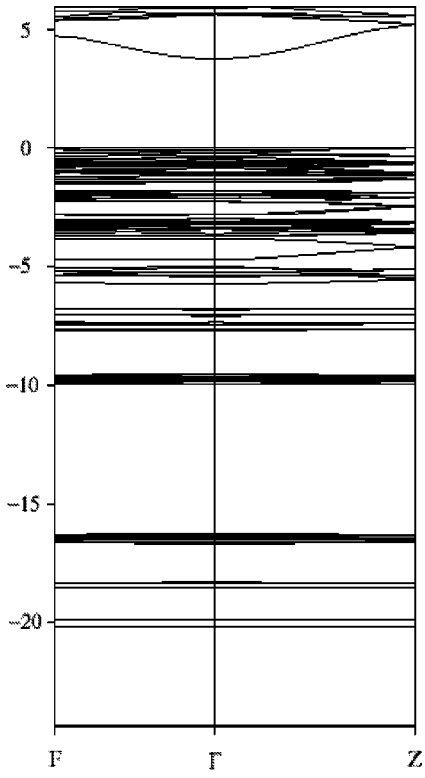

FIG. 1. Band structures of BBO calculated using optimized pseudopotentials.

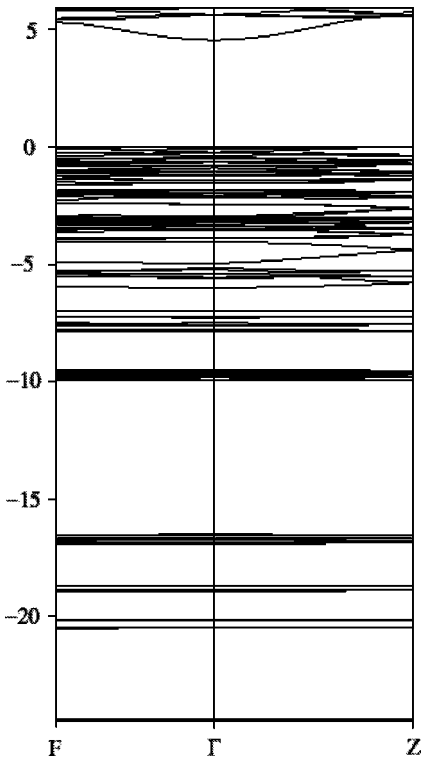

FIG. 2. Band structures of BBO calculated using ultrasoft pseudopotentials.

especially the valence bands. This also indicates the validity of our electronic-structure calculation of BBO.

Li and co-workers have pointed out that the bottom of the conduction band for BBO is primarily composed of Ba $6s$ atomic orbitals.[14] Therefore, they related the band gap of BBO to the transition from the valence orbital of the $(B_3O_6)^{3-}$ group to the Ba $6s$ orbital. Our results for the partial density of states (PDOS) analysis are very similar to theirs in the valence bands, but different in the conduction bands. The DOS of BBO and the PDOS of Ba, B, and O atoms that we obtained are shown in Fig. 3. It is clear in our results that the valence bands of BBO are mainly composed of the $2p$ orbital of B and O atoms in the $(B_3O_6)^{3-}$ group. The $2s$ orbital of the O atom is strongly localized at -20.0 eV, while the $5p$ semicore states of the Ba^{2+} cation are also located in a strongly localized band centered at -10.0 eV. These points are in agreement with the results given by Li (Ref. 14). In contrast to the PDOS given by other authors,[12,14] our results show that there is a strongly localized state at -25 eV, which is projected and shown to be the Ba $5s$ orbital. Its appearance results from the fact that the Ba pseudopotential generated by us takes the Ba $5s$ electrons as valence electrons. Furthermore, Fig. 3 clearly shows that the $2s$ and $2p$ orbitals of B and O atoms strongly contribute to the bottom of the conduction bands, but the density of states at the bottom of the CB is small compared to that of the upper bands. These results have a significant bearing on the optical response. We will discuss this further in Secs. III B and III C.

B. The linear optical susceptibility of BBO

Before analyzing the optical response of BBO, we determine the cutting radius of Ba, B, and O. Figure 4 presents the

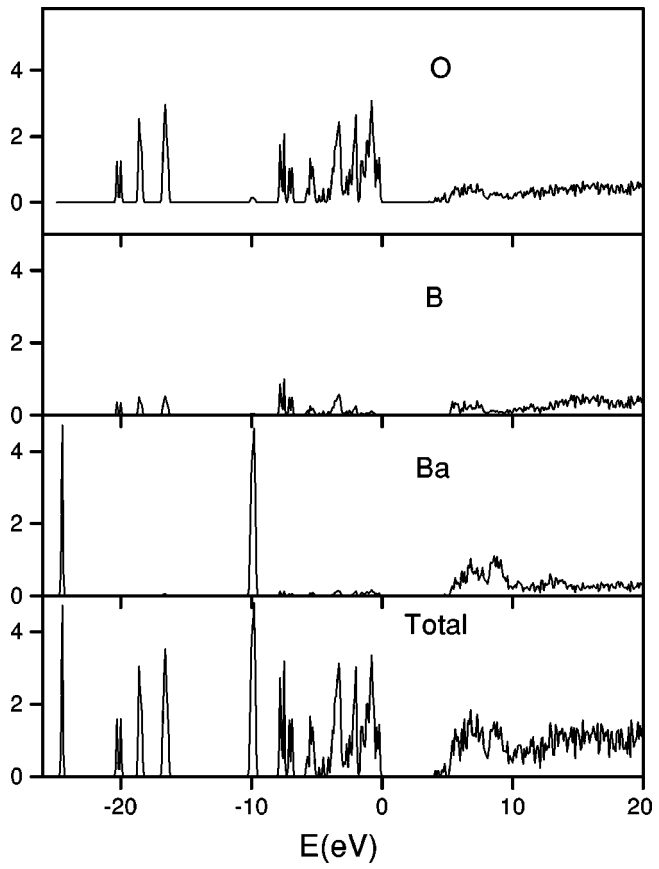

FIG. 3. Total and partial density of states of BBO.

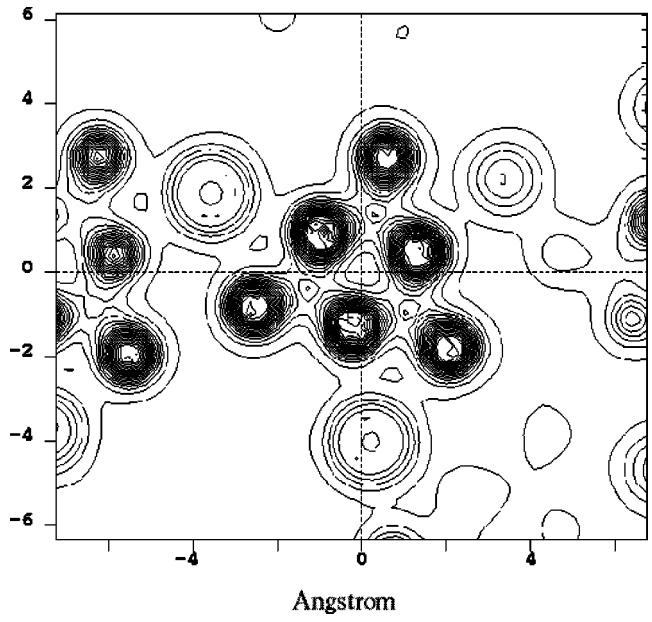

FIG. 4. Charge density in the $(B_3O_6)^{3-}$ group plane. The charge density around the $(B_3O_6)^{3-}$ group is much larger than that around Ba.

charge-density distribution in the plane of the B_3O_6 group. We see that the distance between B and O in the B_3O_6 group is much smaller than the distance between Ba and ions in the B_3O_6 group. We also find that the charge density in the B_3O_6 group is relatively unlocal compared to that of the Ba cation. It is not surprising since the bonding between B and O is more covalent. Therefore, it is difficult to separate the B and O ions and the B_3O_6 group should be treated as a whole. The fact that the charge density around B or O is not very spherelike bewilders one in how to determine their cutting radius clearly. However, considering B and O are cut together, we can allow the overlapping of the cutting spheres for B and O to solve this problem. The overlapping makes it possible to enlarge the cutting radius of B, so that the whole electron subsystem of the B_3O_6 group can be involved in the cutting spheres of B and O.

Since the charge density around Ba is spherelike, we first determine its cutting radius. In accordance with our strategy, presented in Sec. II, we find that the cutting radius of Ba is 1.50 Å by investigating the charge-density distribution between the nearest Ba and O ions. Following to the rule of keeping the cutting spheres of Ba and O in contact and not overlapped, the cutting radius of O is set to be 1.11 Å. Noting that the charge density in the B_3O_6 group is unlocal, we find that the cutting radius of B must be selected as large as possible to ''clear'' the effect of the B_3O_6 group cleanly. Consequently, we choose 0.88 Å, the covalent radius of B, to be its cutting radius. We also found in our calculations that the small changes of cutting radius does not influence the conclusions we are going to make in present work.

In Fig. 5 the calculated dispersion curves of the refractive indexes $n_z(ne)$ and $n_x(=n_y=n_o)$ of the BBO crystal are plotted together with the available experimental data. Calculated and experimental values of refractive indexes and the birefringence at various wavelengths are listed in Table V. All show an excellent agreement between calculation and experiment.

In order to investigate the influence of the ions on the linear optical response of BBO, our real-space atom-cutting method was used. The imaginary part of the dielectric function using various methods of cutting is presented in Fig. 6, where we can see the contributions of various transitions to $\mathrm{Im}[\epsilon(\omega)]$. For example, the contribution of transitions from the B_3O_6 group in the VB to Ba in the CB is achieved by cutting Ba from VB wave functions and cutting the B_3O_6 group from CB wave functions. One can easily see that the summation of contributions from all four types of transitions is in good agreement with the values calculated from uncut wave functions. This fact verifies our assumption that the contribution from the interstitial region is negligible.

In Table VI the contribution of the Ba ion and B_3O_6 group to the anisotropy of BBO is demonstrated. The column entitled ''total'' lists the refractive indexes calculated from the original wave function, while the column entitled ''ion/ion group cut'' means that those values are calculated from the cut-ion/ion group wave functions.

On the basis of the above calculations, we conclude the following:

(i) Calculated refractive indexes (see Table V) are in good agreement (the relative error is less than 3%) with the experimental values. The agreement proves the validity of our treatment of BBO with the pseudopotential based method. The excellent agreement between the experimental and calculated birefringence (error$<$3%) is very helpful to NLO crystal designing.

(ii) Figure 6 shows that the off-site transition is not as important as the on-site transition in the optical response.

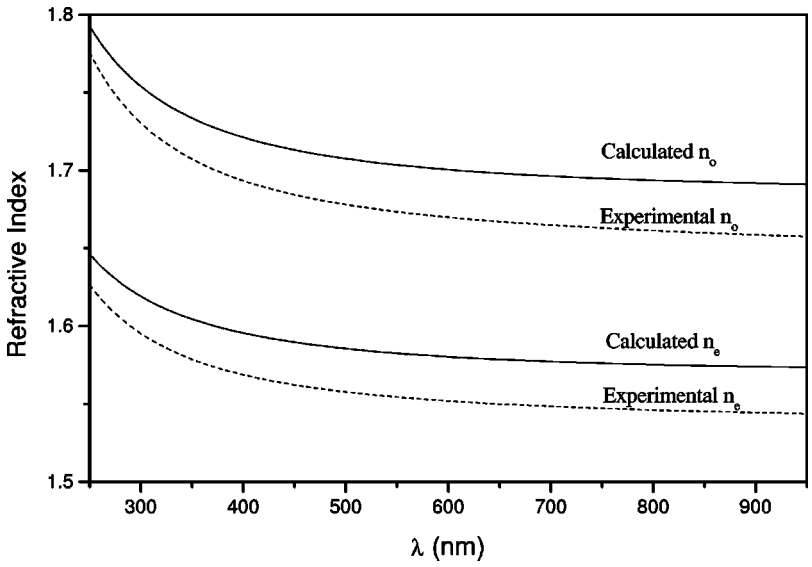

FIG. 5. Calculated and experimental dispersion curve of the refractive indexes of BBO.

This is not surprising, since the charge density of the B-O group is far away from that of Ba. Furthermore, unlike the conclusion derived by Li *et al.*,[14] we find that the slowly varying region near the gap edge (see Fig. 14 in Ref. 14) is not due to the difference between the magnitudes of inter-atomic and intra-atomic transition, because in our calculation the bottom of the conduction band is dominated by (B_3O_6) groups. Furthermore, one can easily see in Fig. 6 that it is the intra-atomic transition within orbitals of the $(B_3O_6)^{3-}$ group that accounts for this slowly varying region near the gap edge. In our opinion, the density of states at the bottom of the CB is too small to contribute much to optical response. One can further find that in on-site transitions the contribution of transitions in the $(B_3O_6)^{3-}$ group is in general larger than that in Ba, because the charge density around Ba is smaller.

(iii) Table VI shows that the contribution of Ba^{2+} to the refractive indexes is about two times smaller than that of the B_3O_6 group, while its contribution to anisotropy is very small. It can be derived that, although Ba^{2+} does contribute to the refractive indexes of BBO, it does not contribute to its anisotropy. These results are consistent with those made by the quantum-chemistry localized model. An intuitive explanation is that although the spherelike cation Ba^{2+} contributes to the values of refractive indexes, its high symmetry indicates that it has almost nothing to do with the anisotropy of the crystal. In other words, the planar $(B_3O_6)^{3-}$ anionic group plays a more important role than the spherelike cations in birefringence.

C. SHG coefficients

Using the Eq. (3a), the SHG coefficients of BBO have been calculated from band wave functions. To test the convergence of the number of k points in the irreducible Brillouin zone for the SHG coefficients, we present in Table VII three sets of the SHG values calculated from 1, 6, and 10 k points in IBZ, respectively. The results from previous calculations as well as experimental values are also shown in Table VII for comparison. To calculate the respective contributions of various processes and transitions to the SHG coefficients of the BBO crystal, the real-space atom-cutting method is adopted again. Table VIII shows clearly the contributions of the Ba^{2+} and $(B_3O_6)^{3-}$ group as well as their joint contribution. For example, the contribution of two states of Ba in the valence band and one state of B_3O_6 group in the conduction band can be obtained from the virtual hole contribution by cutting the B_3O_6 group from the valence-band wave functions and cutting Ba from the conduction-band wave functions.

These calculations lead to the conclusions listed below:

TABLE V. Comparison of the calculated and experimental values of refractive indexes and birefringence of BBO at a few specific wavelengths.

	Experimental[a]			Theoretical		
λ (μm)	n_o	n_e	$\Delta n=\lvert n_o-n_e\rvert$	n_o	n_e	$\Delta n=\lvert n_o-n_e\rvert$
0.404 66	1.692 67	1.567 96	0.124 71	1.719	1.595	0.124
0.467 82	1.681 98	1.560 24	0.121 74	1.710	1.588	0.122
0.508 58	1.677 22	1.556 91	0.120 31	1.706	1.585	0.121
0.579 07	1.671 31	1.552 98	0.118 33	1.701	1.581	0.120
0.643 85	1.667 36	1.550 12	0.117 24	1.698	1.578	0.120
0.852 12	1.659 69	1.545 42	0.114 27	1.692	1.575	0.117
1.014 00	1.656 08	1.543 33	0.112 75	1.690	1.573	0.117

[a]Reference 40.

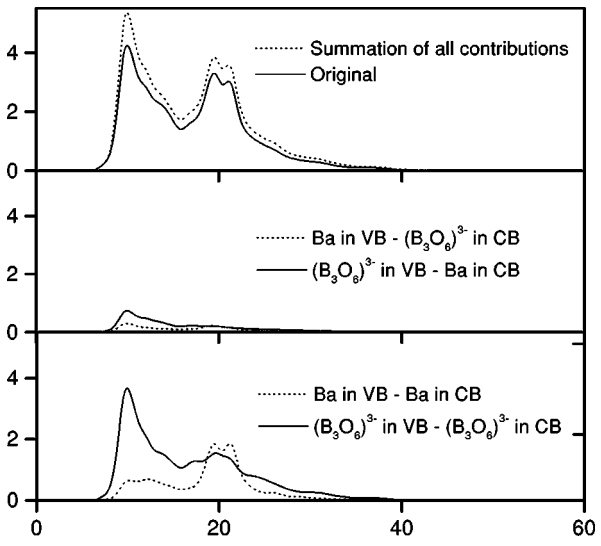

FIG. 6. Imaginary part of the dielectric function. The contributions from various transitions are obtained with our real-space atom-cutting method. The total summation of contributions of all four kinds of transitions are compared with $\epsilon(\omega)$ calculated from original wave functions.

(i) Our planewave pseudopotential approach is suitable for studying the SHG coefficients of BBO. We can see that besides the good agreement of calculated and experimental values of the largest SHG coefficient d_{22}, the other two small coefficients calculated, d_{31} and d_{33}, are in good agreement with the experimental ones, both in absolute value and sign. The deviation of our results from experimental ones and that of linearized augmented plane-wave (LAPW) calculation[15] is in a factor of 2, which is about the same as that in calculations of some semiconductors. On the other hand, the method we previously adopted on the basis of localized molecular orbitals cannot include the contribution of Ba, and therefore cannot give the correct prediction for the two small SHG coefficients. Consequently, the present results show that our method based on the *ab initio* band-structure calculation can certainly give a more complete understanding of the NLO properties of BBO than the localized models.

TABLE VI. Comparison of the refractive indexes and birefringence of BBO at the static limit derived from the cut-Ba wave functions and cut-$(B_3O_6)^{3-}$ group wave functions with the original values.

	Total	Ba cut	$(B_3O_6)^{3-}$ group cut
n_o	1.6851	1.5280	1.2396
n_e	1.5695	1.4114	1.2392
$\Delta n=\lvert n_o-n_e\rvert$	0.1156	0.1166	0.0004

(ii) Because the dimensions of BBO are large ($a=b=c=8.38$ Å), the volume of BZ is very small. Furthermore, the energy band of the crystal is in general narrow. Therefore, a small number of k points is enough for calculating the optical properties of BBO. As a result, the SHG coefficient converges well for $n_{k\ points}=6$.

(iii) Through an analysis of the contributions of the virtual hole and virtual electron processes, we find that since three bands must be considered in the calculation of SHG coefficients, the case becomes much more complex than that in linear optical effects. Contributions of various combinations are listed in Table VIII. We find that generally the virtual electron process contributes more to the total response than the virtual hole process. When calculating d_{22}, we also find that the ''pure'' contribution of the B_3O_6 group (all three states are atomic states of the B_3O_6 group) is three times as much as that of Ba, and is the largest contribution (0.628 pm/V). The second largest individual contribution is also mainly due to the B_3O_6 group, which orginates from a virtual hole process, in which two states in the VB are atomic states of the Ba and B_3O_6 group, respectively, and one state in the CB is a state of the B_3O_6 group. The interatomic transition from a B_3O_6 group state in the VB to a Ba state in the CB is not the dominant source of large d_{22}, because the total contribution of all processes including such transitions is 0.234 pm/V, which is only 17% of the total d_{22}.

In the case of d_{22}, we find that the summation of all calculated contributions is approximately the same as the value calculated from wave functions without cutting. This fact verifies our assumption that d_{22} results mostly from the

TABLE VII. Comparison of the calculated and experimental values of nonlinear susceptibilities of BBO (in pm/V). The number of special k points in the irreducible Brillouin zone for integration is represented as n_k.

	d_{22}	d_{31}	d_{33}
Present calculation			
$n_k=1$	-1.26	0.041	0.020
$n_k=6$	-1.38	0.056	0.0030
$n_k=10$	-1.39	0.058	0.0032
Previous calculations			
LAPW, Duan *et al.*, Ref. 15	-2.98	0.18	0.021
INDO/S-CI, Cheng *et al.*, Ref. 13	-3.51	0.16	
Gaussian'92, Chen *et al.*, Ref. 41	-2.03		
CNDO, Chen *et al.*, Ref. 1	-2.2		
Experimental			
Chen *et al.*, Ref. 3	$\pm 1.60(1\pm 0.05)$	$\mp(0.11\pm 0.05)$	≈ 0
Eckardt *et al.*, Ref. 42	$\pm 2.20(1\pm 0.05)$		

TABLE VIII. Analysis of the SHG coefficients using our real-space atom-cutting method (in pm/V).

Contributions of the virutal hole process				
Valence bands	Conduction bands	d_{22}	d_{31}	d_{33}
Ba and Ba	Ba	−0.122	0.0175	0.0027
Ba and B_3O_6 group	Ba	0.028	0.0068	0.0019
B_3O_6 group and B_3O_6 group	Ba	−0.025	0.0003	0.0009
B_3O_6 group and B_3O_6 group	B_3O_6 group	−0.055	0.0061	0.0051
B_3O_6 group and Ba	B_3O_6 group	−0.177	0.0029	0.0117
Ba and Ba	B_3O_6 group	−0.013	0.0018	−0.0017
Contributions of virtual electron process				
Ba	Ba and Ba	−0.098	0.0041	0.0104
Ba	Ba and B_3O_6 group	0.067	0.0004	0.0007
Ba	B_3O_6 group and B_3O_6 group	−0.026	−0.0015	0.0000
B_3O_6 group	B_3O_6 group and B_3O_6 group	−0.573	0.0022	−0.380
B_3O_6 group	Ba and B_3O_6 group	−0.130	0.0102	0.0368
B_3O_6 group	Ba and Ba	−0.107	−0.0075	−0.0098
Total		−1.231	0.0434	0.0213
Original		−1.38	0.056	0.0030

atomic orbitals of electronic subsystems. In all contributions, that of B_3O_6 group is found to be the dominant origin, and the contribution of Ba is small but cannot be neglected. On the other hand, in the case of d_{33}, the summation of all calculated contributions differs from the value calculated from the original wave functions. Thus, this coefficient comes from unlocal NLO effects and cannot be considered as the simple summation of contributions from local electronic subsystems. In the case of d_{31}, unlocal effects are not dominant but cannot be neglected. Among the local effects in d_{31}, the ''pure'' contribution of Ba is found to be the largest.

(iv) Earlier, we used a localized molecular-orbital method called the anionic group model to calculate the SHG coefficients of BBO.[7] Later, a Gaussian'92 *ab initio* method was also applied to such calculations and more convincing results were achieved.[41] All these calculations based on the localized model indicated that the $(B_3O_6)^{3-}$ anionic group contributes mainly to d_{22}, while the other two small d_{ij} coefficients are primarily produced by the contribution of Ba^{2+} cations. However, the localized feature of the anionic group model could restrict the accuracy of the calculations for SHG coefficients, since it is difficult to take into account both the interaction between Ba^{2+} and the $(B_3O_6)^{3-}$ group and the influence of this interaction on the SHG coefficients. Our present first-principles calculations can overcome these difficulties, and test whether the results obtained by the anionic group model are correct or not. Furthermore, it can give a more detailed explanation of the interactions between the cation and anionic groups. Since the charge densities strongly localize around the B_3O_6 group, it is not surprising that the anionic group contributes more to the optical response than Ba does. Furthermore, in NLO effects, the relatively nonlocal π-conjugate orbital of the B_3O_6 group favors the generation of the largest SHG coefficient of BBO, d_{22}. Hsu and Kasowski[11] suggested that the Ba at the bottom of the CB may contribute much to SHG effects. However, we find in our calculation that the bottom of the CB is mainly composed of O atomic orbitals. Even if Ba atomic orbitals dominate the bottom of CB, the contribution of off-site transitions from the B_3O_6 group in the VB to Ba in the CB does not contribute much to NLO effects, since the off-site transition is generally found to contribute much less than the on-site transition does to optical response. As for the other two small d_{ij} coefficients, since the symmetry of the atomic orbitals of the local electronic subsystem of the B_3O_6 group determines that it contributes very little to them, the contribution of nonlocal effects and Ba atomic orbitals becomes important.

IV. CONCLUSION

An *ab initio* electronic/band-structures calculation has been carried out, using the CASTEP package to investigate the optical properties of BBO from first principles. A formalism for a SHG coefficients calculation based on band structure which explicitly shows the Kleinman symmetry is adopted to calculate the SHG coefficients. Good agreement between experimental and theoretical results is obtained.

A method for analyzing the respective contributions of subsystems to the total optical response is suggested and used to evaluate the role that the Ba^{2+} cation and the $(B_3O_6)^{3-}$ group play in the linear and nonlinear optical properties of BBO. The respective contributions of various manners of transitions to certain optical properties, including dielectric function, refractive indexes, birefringence, and static SHG coefficients, have been calculated. The calculations show that the contribution of the Ba^{2+} cation to the refractive indexes is comparable to that of the B_3O_6 group, whereas its contribution to the birefringence can be neglected. This means that the birefringence of BBO is determined by the $(B_3O_6)^{3-}$ group, which is in agreement with the result obtained by the anionic group model. The contributions of on-site and off-site transitions are explicitly compared, and it is found that on-site transitions generally contribute much more than off-site transtions. Calculations of the SHG coefficients of BBO indicate that d_{22} is also mainly due to the transition within the orbital of the $(B_3O_6)^{3-}$

group, while nonlocal effects and atomic orbitals of Ba are more important factors that influence the other two independent coefficients. We believe that further application of the real-space atom-cutting method may elucidate the origin of the optical effects, both linear and nonlinear, in other borate series NLO crystals, and help us to find and design new NLO crystals more efficiently.

ACKNOWLEDGMENTS

This work was supported by the Chinese National ''Climb-up'' project. Support in computing facilities from the Computer Network Information Center is gratefully acknowledged. The authors thank Dr. Chun-gang Duan for fruitful discussions.

*Present address: Department of Material Science, Mailbox 138-78, California Institute of Technology, Pasadena, CA 91125.

†Present address: Institute f. Geowissenschaften, Kristallographie/ Mineralogie, Univ. of Kiel, Olshausenstr. 40, D-24098 Kiel, Germany.

[1] C. T. Chen, *Development of New Nonlinear Optical Crystals in the Borate Series*, edited by V. S. Letokhov, C. V. Shank, Y. R. Shen, and H. Walther (Harwood Academic, Chur, 1993).

[2] P. Becker, Adv. Mater. **10**, 979 (1998).

[3] C. T. Chen, B. C. Wu, A. D. Jiang, and G. M. You, Sci. Sin. Ser. B **28**, 235 (1985).

[4] C. T. Chen, Y. C. Wu, A. D. Jiang, B. C. Wu, G. M. You, R. K. Li, and S. J. Lin, J. Opt. Soc. Am. B **6**, 616 (1989).

[5] C. T. Chen, N. Ye, J. Lin, J. Jiang, W. Zeng, and B. Wu, Proc. SPIE **3556**, 14 (1998).

[6] C. T. Chen, Acta Phys. Sin. **25**, 146 (1976).

[7] R-K. Li and C. T. Chen, Acta Phys. Sin. (in Chinese) **34**, 824 (1985).

[8] D. E. Ellis and G. S. Painter, Phys. Rev. B **2**, 2887 (1970).

[9] K. Wu and C. T. Chen, J. Cryst. Growth **166**, 533 (1996).

[10] R. H. French, J. W. Ling, F. S. Ohuohi, and C. T. Chen, Phys. Rev. B **44**, 8496 (1991).

[11] W. Y. Hsu and R. V. Kasowski, J. Appl. Phys. **73**, 4101 (1993).

[12] Y-N. Xu, W. Y. Ching, and R. H. French, Phys. Rev. B **48**, 17 695 (1993).

[13] W.-D. Cheng, J.-S. Huang, and J.-X. Lu, Phys. Rev. B **57**, 1527 (1998).

[14] J. Li, C.-G. Duan, Z.-Q. Gu, and D.-S. Wang, Phys. Rev. B **57**, 6925 (1998).

[15] C.-G. Duan, J. Li, Z.-Q. Gu, and D.-S. Wang, Phys. Rev. B **59**, 369 (1999).

[16] CASTEP 3.5 program developed by Molecular Simulations Inc., 1997.

[17] M. C. Payne, M. P. Teter, D. C. Allan, T. A. Arias, and J. D. Joannopoulos, Rev. Mod. Phys. **64**, 1045 (1992).

[18] W. Kohn and L. J. Sham, Phys. Rev. **140**, A1133 (1965).

[19] P. Hohenberg and W. Kohn, Phys. Rev. **136**, B864 (1964).

[20] A. M. Rappe, K. M. Rabe, E. Kaxiras, and J. D. Joannopoulos, Phys. Rev. B **41**, 1227 (1990).

[21] J. S. Lin, A. Qteish, M. C. Payne, and V. Heine, Phys. Rev. B **47**, 4174 (1993).

[22] M-H. Lee, J-S. Lin, M. C. Payne, V. Heine, V. Milman, and S. Crampin (unpublished).

[23] L. Kleinman and D. M. Bylander, Phys. Rev. Lett. **48**, 1425 (1982).

[24] S. G. Louie, S. Froyen, and M. L. Cohen, Phys. Rev. B **26**, 1738 (1982).

[25] See, for example, A. Takada, C. R. A. Catlow, J. S. Lin, G. D. Price, M. H. Lee, V. Milman, and M. C. Payne, Phys. Rev. B **51**, 1447 (1995); K. Refson, R. A. Wogelius, D. G. Fraser, M. C. Payne, M. H. Lee, and V. Milman, *ibid.* **52**, 10 823 (1995); B. Winkler, V. Milman, B. Hennion, M. C. Payne, M. H. Lee, and J. S. Lin, Phys. Chem. Miner. **22**, 461 (1995); I. Dawson, P. D. Bristowe, M. H. Lee, M. C. Payne, M. D. Segall, and J. A. White, Phys. Rev. B **54**, 13 727 (1996); M. H. Lee, C. F. Cheng, V. Heine, and J. Klinowski, Chem. Phys. Lett. **265**, 673 (1997).

[26] A. J. Read and R. J. Needs, Phys. Rev. B **44**, 13 071 (1991).

[27] R. W. Godby, M. Schluter, and L. J. Sham, Phys. Rev. B **37**, 10 159 (1988).

[28] C. S. Wang and B. M. Klein, Phys. Rev. B **24**, 3417 (1981); M. S. Hybertsen and S. G. Louie, *ibid.* **34**, 5390 (1986).

[29] Z. H. Levine and D. C. Allan, Phys. Rev. B **43**, 4187 (1991); J. L. P. Hughes and J. E. Sipe, *ibid.* **53**, 10 751 (1996).

[30] P. N. Butcher and T. P. McLean, Proc. Phys. Soc. London **81**, 219 (1963).

[31] D. E. Aspnes, Phys. Rev. B **6**, 4648 (1972).

[32] E. Ghahramani, D. J. Moss, and J. E. Sipe, Phys. Rev. B **43**, 8990 (1991).

[33] J. E. Sipe and E. Ghahramani, Phys. Rev. B **48**, 11 705 (1993).

[34] C. Aversa and J. E. Sipe, Phys. Rev. B **52**, 14 636 (1995).

[35] Z. H. Levine, Phys. Rev. B **42**, 3567 (1990).

[36] Z. H. Levine and D. C. Allan, Phys. Rev. Lett. **66**, 41 (1991).

[37] Z. H. Levine, Phys. Rev. B **49**, 4532 (1994).

[38] A. Dal Corso and F. Mauri, Phys. Rev. B **50**, 5756 (1994); A. Dal Corso, F. Mauri, and A. Rubio, *ibid.* **53**, 15 638 (1996).

[39] S. N. Rashkeev, W. R. L. Lambrecht, and B. Segall, Phys. Rev. B **57**, 3905 (1998).

[40] V. G. Dimitriev, G. G. Gurzadyan, and D. N. Nikogosyan, *Handbook of Non-linear Optical Crystals*, 2nd revised ed. (Springer, Berlin, 1997).

[41] C. T. Chen, N. Ye, J. Lin, W-R. Zeng, and B-C. Wu, Adv. Materials **11**(13), (1999).

[42] R. C. Eckardt, H. Masuda, Y. X. Fan, and R. L. Byer, IEEE J. Quantum Electron. **26**, 922 (1990).